Study on the Influence of Compaction Degree of Fill behind the Retaining Wall to the Critical Width-Height Ratio of Finite Soil in Active Failure under TT Mode

Xiaohong Liu, Yuchen Liu, Zhengfu Liu, Yongqing Zeng*, *Member, IAENG,* Yuxing Wang, Sanxian Liu

Abstract—**The critical width-height ratio is a crucial parameter for defining the fill behind the wall as finite soil. Most existing studies on the critical width-height ratio of finite soil use loose sand as filler, without considering the influence of fill compaction degree on the critical width-height ratio of finite soil. By using of model test and numerical simulation, this paper studies the influence of compaction degree of fill behind the retaining wall on the active failure characteristics and the critical width-height ratio of finite soil under TT mode. The empirical relation between compaction degree and density, as well as the compaction degree and internal friction angle of fill materials is established through geotechnical tests. The dynamic development law on active fracture surface of the soil filling with different compaction degrees and width-height ratios behind the retaining wall is obtained. The method of determining the critical width-height ratio of the finite soil mass based on the morphological characteristics of fracture surface is proposed. The empirical formula of the critical width-height ratio of finite soil mass considering the compaction degree of fill is given. Under the TT mode, for the finite soil, the active fracture surface is a multi-segment broken line, starting from the heel of the movable retaining wall and going back and forth between the fixed retaining wall and the movable retaining wall, and ending at the fill surface; for the semi-infinite soil, the active fracture surface is an approximate straight line from the wall heel to the fill surface. For finite soil with a certain width-height ratio, with the increase of compaction degree, the active fracture surface gradually changes from a broken line to a straight line; the finite soil gradually becomes semi-infinite soil. For semi-infinite soil with a certain width-height ratio, with the increase of the compaction degree, the active fracture surface gradually becomes steeper, and the volume of the broken body gradually decreases; the soil behind the wall is still semi-infinite. When the compaction degree is constant, with the increase of the width-height ratio, the active fracture surface gradually changes from a broken line to a straight line, and the finite soil behind the wall gradually changes to semi-infinite soil. Under the TT mode, the active failure critical width-height ratio of finite soil decreases linearly with the increase of the compaction degree of fill, showing a highly linear correlation. The compaction degree of backfill is one of the important factors affecting the critical width-height ratio, which should be considered in the design and construction of actual support engineering. The study is of great significance for determining the critical width-height ratio of finite soil behind the retaining wall, and can provide a reference for the deformation analysis and earth pressure calculation of the finite soil behind the retaining structure.**

Index Terms—**Critical width-height ratio, Compaction degree, Finite soil, TT mode, Active fracture surface**

Manuscript received August 20, 2024; revised February 13, 2025. The study was supported by the Natural Science Foundation of Hunan Province of China (Grant No. 2022JJ40160), the Key Scientific Program of Hunan Education Department, China (Grant No. 22A0472), and the Postgraduate Scientific Research Innovation Project of Hunan Province, China (Grant No. CX20231231).

Xiaohong Liu is a professor in College of Civil Engineering and Architecture, Hunan Institute of Science and Technology, Yueyang, 414000 China. (e-mail: 11991491@hnist.edu.cn).

Yuchen Liu is a postgraduate student in College of Civil Engineering and Architecture, Hunan Institute of Science and Technology, Yueyang, 414000 China. (e-mail: 1453837198@qq.com).

Zhengfu Liu is a lecturer in College of Management, Hunan City University, Yiyang, 413000 China. (e-mail: 597073225@qq.com).

Yongqing Zeng is an associate professor in College of Civil Engineering and Architecture, Hunan Institute of Science and Technology, Yueyang, 414000 China. (corresponding author to provide e-mail: yqzeng@hnist.edu.cn).

Yuxing Wang is a postgraduate student in College of Civil Engineering and Architecture, Hunan Institute of Science and Technology, Yueyang, 414000 China. (e-mail: wangyuxin990928@163.com).

Sanxian Liu is a registered geotechnical engineer in Yueyang Baili Survey Technology Co., Ltd. of Hunan Province. Yueyang, 414000 China. (e-mail: 330224270@qq.com).

I. Introduction

THE classical earth pressure theory assumes that the fill behind the slope retaining wall is a semi-infinite soil, the fracture surface is a plane from the heel of the wall to the surface of the fill [1-3]. With the rapid development of urbanization construction, urban land is becoming increasingly tense. The density of ground and underground structures is increasing, in the process of foundation pit excavation, the phenomenon of retaining walls near existing underground structures has become normal [4-6]. The schematic diagram of finite soil is shown in Fig. 1, due to the obstruction of near the underground structure, the fracture surface cannot directly reach the ground surface, which does not conform to the assumption of semi-infinite soil in the classical earth pressure theory. At the moment, the finite width soil between the foundation pit supporting structure and the adjacent underground structure is called finite soil.

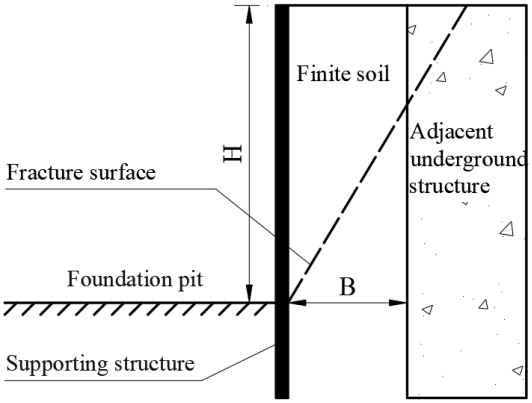

Fig. 1. Schematic diagram of finite soil.

At present, there is no unified standard for calculating the earth pressure of finite soil behind the retaining wall, and the existing calculation theory of finite soil pressure lags behind the rapid development of engineering practice [7-8]. It is necessary to study the earth pressure, deformation rule and failure mechanism of finite soil. Due to the different calculation methods of earth pressure between semi-infinite soil and finite soil, before calculating the earth pressure, it should be judged whether the backfill behind the retaining wall is semi-infinite soil or finite soil. In most existing literature, the width-height ratio of fill is used to define finite soil [9-10], the schematic diagram of critical width-height ratio of finite soil is shown in Fig. 2, when the fractured surface of the backfill behind the wall passes through the intersection point of the backfill surface and the adjacent underground structure outer wall surface, the corresponding width-height ratio (n) of fill is the critical width-height ratio (n_{cr}) of finite soil, $n_{cr}=B/H$, when $n \le n_{cr}$, the fill behind the retaining wall is called finite soil.

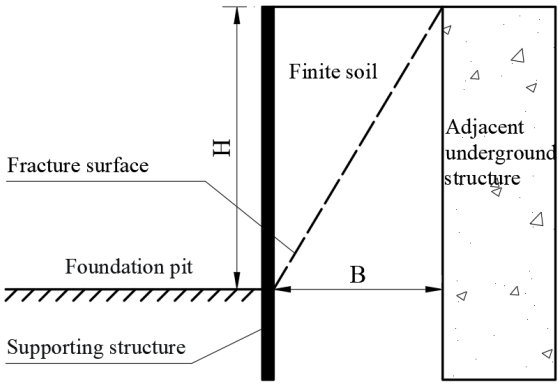

Fig. 2. Schematic diagram of critical width-height ratio of finite soil.

According to the existing literature, the research on finite soil is mainly carried out through model test, numerical simulation, and theoretical analysis.

In terms of model test, as shown in Fig. 3, the three typical active displacement modes of rigid retaining wall are translation mode (TT mode), rotating around top mode (RT mode) and rotating around base mode (RB mode), respectively. Through model test, Dai [11] studied the deformation failure mode and active earth pressure distribution law of loose sand under the TT mode, RT mode and RB mode of retaining wall. The test results show that the critical width-height ratio (n_{cr}) of loose sand under the above three deformation modes is 0.43, 0.44 and 0.35, respectively. Based on DIC technology and image analysis software, Wang [12] used the model test device to carry out the active failure model test of loose sand, and obtained the active deformation rule and the morphological characteristics of fracture surface of loose sand with different width-height ratio under three displacement modes; The critical width-height ratio (n_{cr}) of loose sand under TT mode and RB mode is less than 0.6, and the critical width-height ratio (n_{cr}) of loose sand under RT mode is less than 0.35. Yang [13] carried out the active failure model test under TT mode of saturated sand behind the retaining wall, and obtained the active deformation, failure characteristics and the active earth pressure distribution law of saturated sand; The critical width-height ratio of finite soil under TT mode is slightly less than 0.5. Jiang [14] conducted active failure model tests under three displacement modes, and obtained that the critical width-height ratio (n_{cr}) of loose sand under TT mode, RT mode and RB mode is 0.6, 1.0 and 0.5, respectively. Through active failure model tests of loose sand with different width-height ratio, Yang [15] obtained the morphological characteristics of the active fracture surface of loose sand behind the wall under TT mode; and its critical width-height ratio (n_{cr}) is 0.43. Xia [16] carried out active failure model tests under TT mode with different width-height ratio, and obtained the morphological characteristics of the active fracture surface of loose sand; the analysis shows that the critical width-height ratio (n_{cr}) is between 0.4 and 0.5. Through model test, Fang [17] studied the active failure mode and earth pressure distribution characteristics of loose sand under three displacement modes of retaining wall; the distribution law of earth pressure is different under three different displacement modes, in addition, the calculation results of limit equilibrium method are different from the test results, and the maximum difference is 6.1%. Based on model tests and particle image velocity measurement techniques, Khosravi [18] obtained the deformation and failure characteristics of non-cohesive soil behind the retaining wall, and the distribution law of active earth pressure under TT mode; The good agreement between the experimental results and the arch-action-based theories for lateral active earth pressure could confirm the arching effect behind the retaining walls in the active translation mode. Zhou [19] carried out an experimental study on the active earth pressure of finite soil behind the wall under TT mode with loose sand and cohesive soil, and discussed the distribution law and influencing factors of active earth pressure. Through model test, Zhu [20] studied the active deformation and failure characteristics of loose sand with different width-height ratio (n) under TT mode; the test results show that with the decrease of the width-height ratio of fill, the active fracture surface gradually becomes steeper; The distribution of earth pressure is greatly affected by the displacement and width-height ratio, and the active earth pressure increases along the depth of the retaining wall, showing a nonlinear distribution.

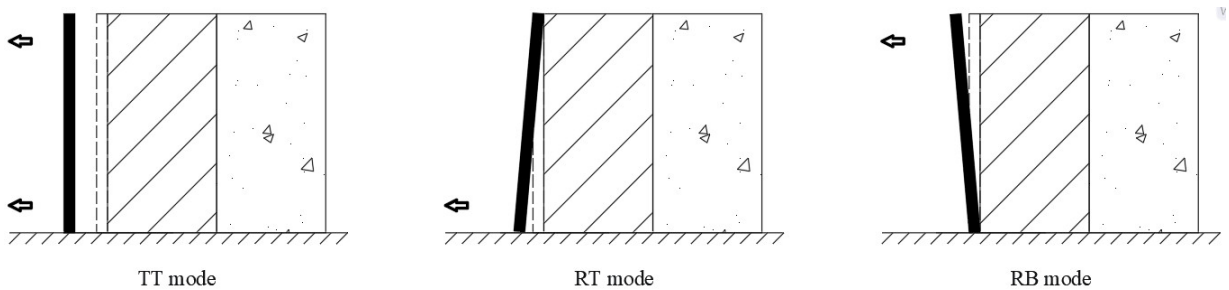

Fig. 3. Schematic diagram of three active displacement modes of retaining wall

In terms of numerical simulation, Liu [21] conducted a numerical model using the discrete element method, and obtained the influence of the width-height ratio of fill on active deformation and fracture surface morphological characteristics under three displacement modes. The results show that the critical width-height ratio (n_{cr}) of loose sand under TT mode is about 0.59. Through discrete element modeling analysis, Wan [22] obtained the active deformation law and failure surface characteristics of the fill under the TT mode. When the wall is smooth, the critical width-height ratio of loose sand is 0.4, the fracture surface of semi-infinite soil is a straight line, and the fracture surface of finite soil is a broken line; when the wall is rough, the critical width-height ratio is 0.6, the semi-infinite fracture surface is curved. With the increase of the roughness of the wall, the reflection phenomenon of the fracture surface of finite soil decreases; with the increase of the width-height ratio, the inclination of the fracture surface decreases. Zhang [23-25] used the discrete element method to conduct modeling and analysis, and obtained the active deformation and failure characteristics of loose sand and the distribution law of earth pressure with different width-height ratios under three displacement modes of retaining walls, the critical width-height ratio is about 0.7 under TT mode. Huang [26] used the numerical calculation software ABAQUS to conduct modeling and analysis, and obtained the active deformation rules and earth pressure distribution characteristics of non-cohesive soil with different width-height ratios under three displacement modes of retaining walls. The results show that the distribution of active earth pressure, the coefficient of active earth pressure, and the position of combined force are related to the displacement mode of retaining wall and the width-height ratio of fill. By establishing and analyzing the discrete element numerical model, Chen [27] obtained the influence law of the friction angle between wall and soil and the width-height ratio of fill on the morphological characteristics of the active fracture surface of non-cohesive soil under the TT mode. When the friction angle between the wall and soil is 25°, the critical width-height ratio of loose sand is 1.5. By means of numerical simulation and physical model test, Du [28] obtained the stability of the land-slide and the distribution law of earth pressure behind the wall under different rainfall working conditions; under the action of continuous heavy rainfall, the earth pressure increases significantly compared with the natural state, the plastic zone of the slope gradually develops until a cut-through sliding surface is formed, and the horizontal displacement of the slope increases sharply, the sliding failure occurs.

In terms of theoretical analysis, by considering the influence of the minor principal stress trajectory, Jiang [29] established an active earth pressure calculation model for finite soil; When the width-height ratio of fill behind a wall is the critical width-height ratio, the inclination angle of the sliding surface $\theta_{cr}=arctan[tan\varphi+(tan^2\varphi+tan\varphi/tan(\varphi+\delta))^{0.5}]$, where φ is the internal friction angle of fill and δ is the friction angle between wall and soil. Based on the limit equilibrium theory and the assumption of plane fracture surface, Ma [30] established the calculation model and derived the calculation expression of finite width cohesive soil earth pressure, the fracture angle of finite soil was affected by the width-height ratio, internal friction angle and cohesion of soil. Liu [31] assumed that the active fracture surface of non-cohesive soil under the TT mode is a plane and the arch of minor principal stress is a circular arc, established a finite soil active earth pressure calculation model and derived the calculation formula. With the increase of width-height ratio n, the active earth pressure gradually increases, the curve of earth pressure distribution becomes more and more nonlinear, the height of resultant force application point gradually decreases, and it is always greater than H/3. It tends to be stable when n is greater than 0.71, so n = 0.71 can be assumed as the critical width-height ratio of finite soil and semi-infinite soil. Lai [32] divided the finite soil under the TT mode into the upper non-slip zone and the lower slip zone; The active earth pressure in the non-slip zone is solved by introducing a curved soil-layer element, and the active earth pressure in the slip zone is obtained by using the limit equilibrium method of the sliding wedge and the finite difference method. Shu [33] assumed that the sliding body and retaining wall are homogeneous rigid body, established a finite soil active earth pressure calculation model for unsaturated cohesive soil, and derived the calculation formula on active earth pressure of finite soil, when B/H is greater than 0.6, it can be regarded as the active earth pressure of infinite soil. Based on the limit equilibrium method and thin layer element method, Wei [34] established a finite soil pressure calculation model and derived the calculation formula of finite soil pressure. Taking into account factors such as cohesion, internal and external friction angles, the calculation theory is more comprehensive and has stronger applicability.

In summary, the critical width-height ratio of finite soil behind the retaining wall is affected by many factors, such as the displacement mode of retaining wall, the type of earth pressure, the kind of fill, and the friction angle between the wall and the soil. Under the active limit failure state in TT mode, the critical width-height ratio of finite soil mainly varies between 0.4 and 0.7. In the existing studies, most of the fill behind the wall is loose sand, which does not consider the requirement of the compaction degree of fill in the actual slope retaining engineering, and does not consider the influence of the compaction degree of the fill on the critical width-height ratio of finite soil. The conclusions obtained from the above studies cannot directly guide the engineering practice. Therefore, it is necessary to consider the influence of compaction degree in the study of the critical width-height ratio of finite soil.

Through model test and numerical simulation, this paper conducts a study on the active failure critical width-height ratio of finite soil under TT mode. The influence of the compaction degree of fill on the characteristics of active fracture surface and the critical width-height ratio of finite soil is revealed; the empirical formula of the critical width-height ratio of finite soil considering the compaction degree of fill is given. The results can further enrich the active earth pressure calculation theory of finite soil, and provide valuable reference for the design and construction of finite soil support structures, which have important theoretical value and engineering practical significance.

II. Test of Physical and Mechanical Properties of Fill

A. Physical Index Test of Fill

The filler used in the test is non-cohesive sand, which is taken from the East Dongting Lake in Yueyang, China. The raw materials are screened to remove pebbles and other impurities, washed with water, and dried in the sun for later use. The particle grading analysis of the fill is shown in Fig. 4, the particle size is mainly concentrated between 0.5mm and 2mm, the non-uniformity coefficient C_u=2.9, and the curvature coefficient C_c=1.4, the fill is coarse sand with poor gradation.

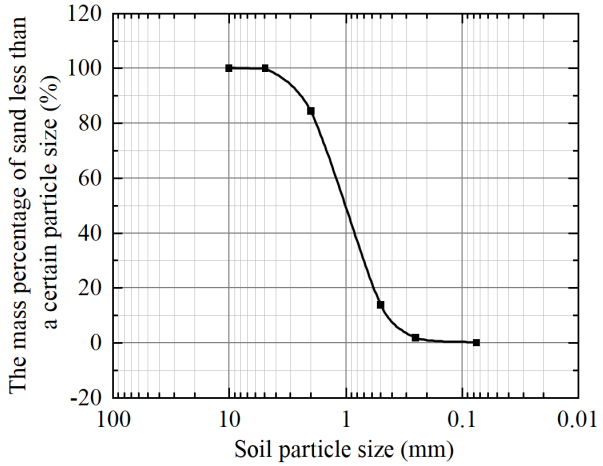

Fig. 4. Particle grading curve of filled sand

The test results show that the air-dried moisture content (ω) of the fill is 1.8%, and the maximum dry density (ρ_{dmax}) is 1.72g/cm^3. Under the condition of free falling sand, the density (ρ_0) of the filler is 1.41 g/cm^3, the dry density $\rho_{d0}=\rho_0/(1+\omega)$ = 1.39 g/cm^3, and the compaction degree λ=80.8%.

B. Test on Relationship between Compaction Degree and Density of Fill

In order to reduce the complicated weighing and calculation work in the subsequent model tests, before the formal model test, it is necessary to obtain the relationship between compaction degree (λ) and density (ρ) of the fill. In order to obtain different compaction degrees of fill soil, the designed impact number N of gravity hammer is 0, 1, 3, 5, 10, 20, 30, 40, 50, 60, and 70, respectively.

1) Test Methods

a) Using the filling box of the model device (Fig. 5) as the filling container, the fixed retaining wall is moved to form a cuboid filling space with a size of 40 cm× 20 cm × 40 cm, and the fill volume (V) is 32000 cm^3.

b) The sand was filled in 4 layers with a thickness of 10 cm per layer. Based on experimental experience and different impact times, before hammering, the layer thickness of the virtual paving is about 11~13cm. Take the N=10 hits as an example to illustrate: The first layer of sand with a thickness of about 12cm is evenly laid at the bottom of the box, and a steel plate with a size of 39cm× 19cm × 2cm is placed on it, and the steel plate is continuously impacted with a 10kg gravity hammer for 10 times. Remove the steel plate, use the brush to roughen the surface of the first layer, flatten it to a 10cm thick scale line, and finally lay a black sand line near the glass (Fig. 5) to complete the laying of the first layer sand. In the same way, lay the 2nd~ 4th layer in turn.

c) Open the sand leakage hole at the bottom of the box, remove the sand from the filling box, and weigh sand mass (m). Then, the density ρ of sand under the corresponding impact number N can be calculated according to $\rho=m/V$.

2) Test Results

The dry density of fill under different impact number N is calculated by $\rho_d=\rho/(1+\omega)$, and the corresponding compaction degree is calculated by $\lambda=\rho_d/\rho_{dmax}$.

The density, dry density and compaction degree of fill under different impact numbers is shown in TABLE I, the compaction degree λ and density ρ are fitted, and the fitting relationship is shown in Eq. (1). It can be seen that the density of fill increases linearly with the increase of compaction degree, and the correlation degree R^2=0.999, showing a high linear correlation.

$$\rho = 0.0174\lambda - 0.0088 \quad R^2 = 0.999 \tag{1}$$

TABLE I
THE DENSITY, DRY DENSITY AND COMPACTION DEGREE OF FILL UNDER DIFFERENT IMPACT NUMBERS

Impact number N	Density ρ/(g/cm^3)	Dry density ρ_d /(g/cm^3)	Compaction degree λ/(%)
0	1.41	1.39	80.8
1	1.45	1.42	82.6
3	1.47	1.44	83.7
5	1.50	1.47	85.5
10	1.53	1.50	87.2
20	1.62	1.59	92.4
30	1.67	1.64	95.3
40	1.70	1.67	97.1
50	1.72	1.69	98.3
60	1.73	1.70	98.8
70	1.73	1.70	98.8

C. Test on Relationship between Fill Compaction Degree and Internal Friction Angle

In order to facilitate the numerical simulation process of determining the values of the internal friction angle of fill soil with different compaction degrees, an experiment was conducted to investigate the relationship between the compaction degree of fill soil and the internal friction angle. Design direct shear tests with compaction degrees λ of 80.8%, 83.7%, 87.2%, 95.3%, and 98.3%, respectively.

1) Test Methods

Taking the direct shear test of fill with compaction degree λ=87.2% as an example, the test operation and steps are described as follows:

a) According to Eq.(1), when the compaction degree λ=87.2%, the sand density ρ=1.508 g/cm^3, the volume in the direct shear box is 60cm^3, and the corresponding sand mass can be calculated to be 90.5g.

b) Weigh 90.5g of sand into the shear box and compact it; the sample's surface is aligned with the 2cm scale line of shear box. Cover the load plate and push the shear box into the compression frame.

c) Zero the dial indicator pointer, apply 100kPa vertical

pressure on the load plate, remove the fixed latch of direct shear box, rotate the hand wheel, apply the shear force in the horizontal direction until the shear failure of sample, record the maximum reading of dial indicator pointer before the shear failure of sample.

d) Reverse the hand wheel to restore the straight shear box to the original position, remove the vertical pressure, remove the soil sample, and clean the shear box.

e) Repeat the above steps, apply vertical pressures 200kPa, 300kPa, and 400kPa, respectively, for the second to fourth samples (each sample with a mass of 90.5*g*), and record the maximum reached by the dial indicator pointer before the shear failure of sample.

f) According to the Coulomb strength theory, the internal friction angle of the fill is 37.8° when $\lambda = 87.2\%$ by using four sets of direct shear test data.

2) Test Results

According to the above method, the internal friction angles of sand with different compaction degree can be obtained, as shown in TABLE II.

By fitting the data in TABLE II, the relationship between compaction degree λ and internal friction angle φ is obtained, as shown in Eq. (2).

$$\varphi = 0.466\lambda - 3.006 \quad R^2 = 0.990 \tag{2}$$

It can be seen from Eq. (2) that the internal friction angle of the fill increases linearly with the increase of compaction degree, and the correlation degree R^2=0.990, showing a high linear correlation.

TABLE II
INTERNAL FRICTION ANGLE OF FILL WITH DIFFERENT COMPACTION DEGREE

Compaction degree λ /(%)	80.8	83.7	87.2	95.3	98.3
Internal friction angle φ/(°)	34.9	35.6	37.8	41	43.1

III. MODEL TEST

A. Model Test Device

The model test device (see Fig. 5) consists of a filling box, a movable retaining wall, a fixed retaining wall, a movable retaining wall displacement control system, and an image acquisition and processing system. The filling box is a steel structure cuboid with a length, width, and height of 1200mm, 400mm, and 700mm, respectively. The front of the box is 16mm thick transparent tempered glass to realize real-time observation, dynamic photography, and later analysis during the test.

The movable retaining wall is made of 16mm thick steel plate, and the upper and lower sides of the steel plate are welded with hinged supports, which are respectively hinged to the upper and lower transmission shafts. The fixed retaining wall is a 12mm thick steel plate. In order to achieve different filling widths, a fixed slot is set every 10cm in the box to place a fixed retaining wall.

The movable retaining wall displacement control system is composed of two sets of three-phase asynchronous motors with the same performance, gear drive shaft, electric control box, and fixed motor support. The power propulsion speed is 0.02mm/s, and three kinds of retaining wall displacement modes can be realized. When motor 1 and motor 2 move to the left at the same time, TT mode under active condition can be realized. When motor 1 is stationary and motor 2 moves to the left, RT mode under active condition can be realized. When motor 1 moves left and motor 2 is stationary, RB mode under active condition can be realized. The above three displacement modes can be controlled by buttons on the control box.

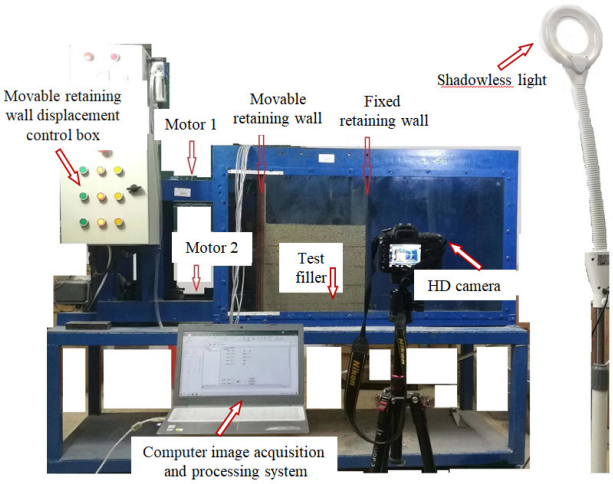

Fig. 5. Test device

The image acquisition and processing system is composed of a high-definition digital camera, shadowless light source, computer, and data processing software, which completes continuous photography, image acquisition, and processing analysis. In this paper, digital image correlation (DIC) technology and image analysis software Geo-PIV are used to process and analyze continuous photos to realize the non-contact measurement of soil deformation. DIC technology is a non-contact, modern optical deformation measurement technology. Its basic principle is to obtain the displacement vector of the point by tracking the position of the same pixel in the two adjacent images during the deformation of the object surface, and then obtains the displacement field and strain field of the surface. Geo-PIV is a non-commercial image analysis and processing software, which has been widely used in non-contact deformation measurement of soil in geotechnical tests.

B. Test Scheme

In order to explore the influence of compaction degree on the critical width-height ratio of finite soil under TT mode, the model test scheme is designed. As shown in TABLE III, according to the previous model test experience, each compaction degree is designed to correspond to 5 different width-height ratios. The compaction degree is set to 81%, 84%, 87%, 90% and 93%, respectively; the five width-height ratios corresponding to each compaction degree of fill soil are 0.2, 0.3, 0.4, 0.5, and 0.6, respectively.

C. Test Methods

Taking the working condition with compaction degree λ=87% and width-height ratio n=0.5 (width of 20cm, height of 40cm) as an example, the specific operation step of model test is introduced:

1) Test preparation: Adjust the movable retaining wall to the initial position; insert the fixed retaining wall into the

TABLE III
ACTIVE FAILURE MODEL TEST SCHEME UNDER TT MODE

Compaction degree λ/(%)	Width-height ratio n
81	0.2, 0.3, 0.4, 0.5, 0.6
84	0.2, 0.3, 0.4, 0.5, 0.6
87	0.2, 0.3, 0.4, 0.5, 0.6
90	0.2, 0.3, 0.4, 0.5, 0.6
93	0.2, 0.3, 0.4, 0.5, 0.6

appropriate slot, so that the net distance between the movable retaining wall and the fixed retaining wall is 20cm. The high-definition camera, shadowless light, and computer are arranged in a suitable position, and the camera shooting frequency is set to 0.5seconds/piece.

2) Sand filling: filling soil in 4 layers, each layer thickness of 10cm. According to Eq.(1), when compaction degree λ=87%, the corresponding density is 1.505g/cm^3, and the mass of sand is 12.04kg per 10cm thickness soil layer. Weigh 12.04kg sand and pour it into the first layer. After leveling, a steel plate with a size of 39cm × 19cm × 2cm is placed on it, and the steel plate is continuously impacted with a 10kg gravity hammer until the thickness of 12.04kg sand is just 10 cm. Remove the steel plate, and lay a black sand line near the glass. Use the same method to lay the 2nd ~ 4th layer until the test soil height reaches 40cm.

3) The test conducting: Close the indoor curtains and turn on the shadowless lamp. Through the button on the control box, the displacement mode of the active retaining wall is set to TT mode. During the displacement process of active retaining wall, the camera takes pictures synchronously and stores them in the computer.

4) Test ending: when the color sand line in the box has obvious dislocation, the test is terminated.

5) Photo processing and analysis: The photos are imported into Geo-PIV software for digital processing and analysis, the dynamic development process of the shear strain cloud map of soil behind the wall is obtained. Then, according to the cloud map and the fault characteristics of black sand line, the region of the active fracture zone is judged. According to whether the fracture surface intersects with the fixed retaining wall, whether the fill is finite soil is judged.

IV. NUMERICAL SIMULATION

Due to the long period, the complicated operation steps and heavy workload of model test, the model test of some working conditions cannot be completed. Therefore, this paper uses the finite element software PLAXIS^{2D} to carry out 1:1 modeling analysis of each working condition (including completed working condition and unfinished working condition) in the model test scheme.

A. Establishment of Finite Element Model

In this paper, the finite element model is established according to the plane strain problem. Taking the working condition of compaction degree λ=84 %, width-height ratio n=0.4 as an example, the establishment of the finite element model is shown in Fig. 6. It is assumed that both the movable retaining wall and the fixed retaining wall are upright rigid body, and the friction angle between retaining wall and the fill is the same, and the surface of the fill behind the wall is horizontal. The rigid retaining wall on both sides adopts the linear elastic model; the soil constitutive relation adopts the Mohr-Coulomb model. The interface element is used to simulate and define the interaction between the retaining wall and the fill, the rigid retaining wall adopts the plate element, and the soil element adopts the 15-node triangular element, the finite element mesh of filling is shown in Fig. 7. A leftward displacement is applied to the active retaining wall to realize the TT mode of retaining wall. The bottom of the model and the fixed retaining wall are fully constrained, and the moving retaining wall is constrained in the Y direction.

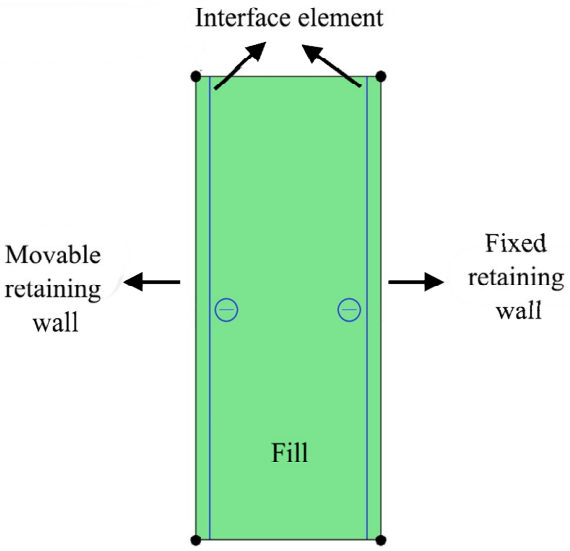

Fig. 6. Finite element model diagram

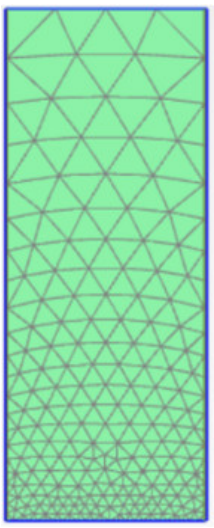

Fig. 7. Finite element grid layout of filling

B. Material Parameters

In the numerical simulation calculation, by adjusting the internal friction angle, density, and width of the fill, the influence of compaction degree and width-height ratio of fill on the active deformation and failure of the soil under the TT mode is studied. The density and internal friction angle of fill with different compaction degree are calculated by using Eq. (1) and Eq.(2), the density is converted into unit weight. The parameters of retaining wall and fill in the finite element model are shown in TABLE IV and TABLE V, respectively.

TABLE IV
PARAMETERS OF RETAINING WALL

Plate type	Density (kN/m^3)	Flexural rigidity ($kN \cdot m^2/m$)	Normal stiffness (kN/m)	Permeable water
Rigid plate	78.5	1×10^6	7.5×10^6	waterproof

TABLE V
PARAMETERS OF FILL

Compaction degree /(%)	Unit weight (kN/m^3)	Internal friction angle (°)
81	14.01	34.7
84	14.53	36.1
87	15.05	37.5
90	15.57	38.9
93	16.09	40.3

V. RESULTS ANALYSIS

A. Dynamic Development Law and Morphological Characteristics of Active Fracture Surface

Taking the working condition with compaction degree λ=81% and width-height ratio n=0.2 as an example, the dynamic development process of the active failure surface of finite soil under TT mode is shown in Fig. 8.

It can be seen from Fig. 8 that the test results of the active fracture surface of finite soil under the TT model are basically consistent with the simulation results, both of which start from the heel of wall and return to the broken line between the fixed retaining wall and the movable retaining wall, and end at the surface of the fill. The fracture surface is composed of three sections. The first section of the fracture surface is formed in the early stage of development, which begins at the heel of the movable retaining wall and ends at about 3/5 of the wall height of fixed retaining wall. The second section of the fracture zone formed in the middle stage begins at about 3/5 of height of the fixed retaining wall and ends at about 9/10 of the height of movable retaining wall, at the moment, the shear strain of the first section increases. At the end, the third section of the fracture zone begins at about 9/10 of the wall height of movable retaining wall and ends at the upper surface of the soil. At the same time, the shear strain of the first and second sections increases accordingly.

Taking the working condition with compaction degree λ=93% and width-height ratio n=0.3 as an example, the dynamic development process of the active fracture surface of semi-infinite soil in TT mode is shown in Fig. 9.

It can be seen from Fig. 9 that with the increase of the displacement of active retaining wall, the first bottom-up color sand line first breaks at the fracture surface, and then the second and third color sand lines successively break, and the breaking distance gradually increases. The test results of the active fracture surface of semi-infinite soil under the TT mode are basically consistent with the simulation results, the active fracture surface all begin at the heel of the wall, then gradually develop upward along the diagonal, and finally end at the surface of fill, the fracture surface is approximately a straight line.

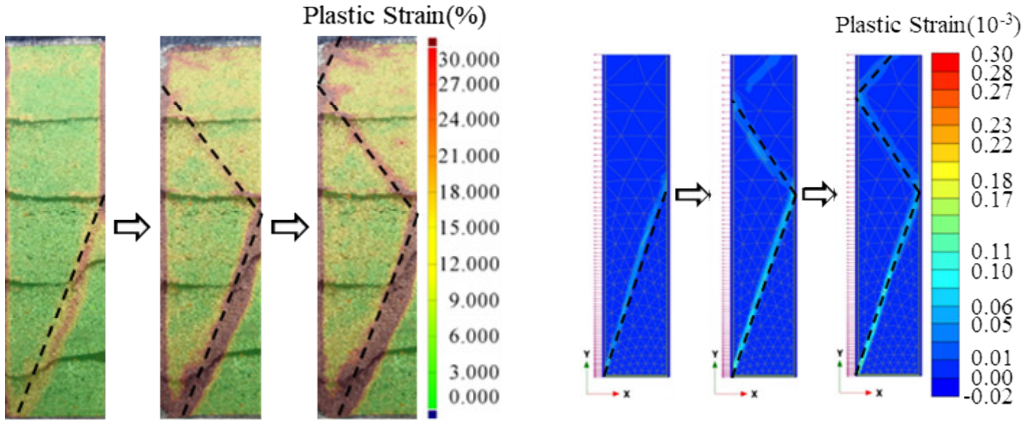

(a) Test results (b) Simulation result

Fig. 8. Dynamic development process of finite soil active fracture surface(λ=81%, n=0.2)

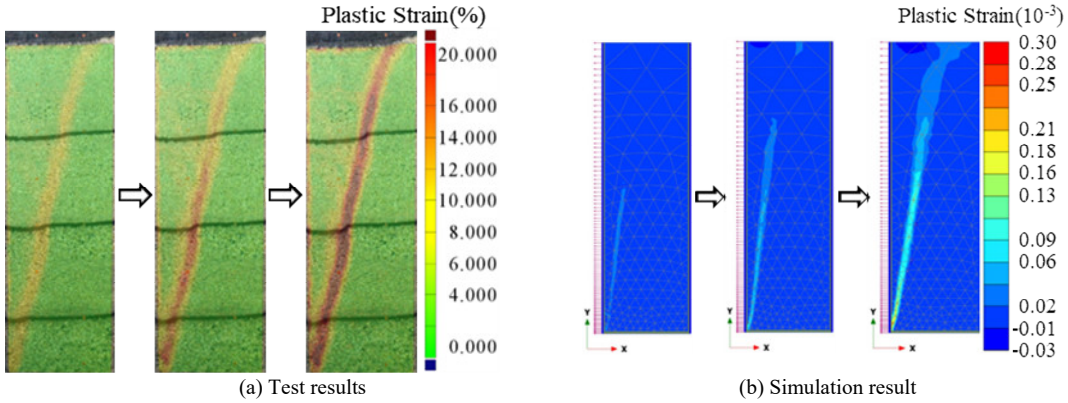

(a) Test results (b) Simulation result

Fig. 9. Dynamic development process of semi-infinite soil active fracture surface (λ=93%, n=0.3)

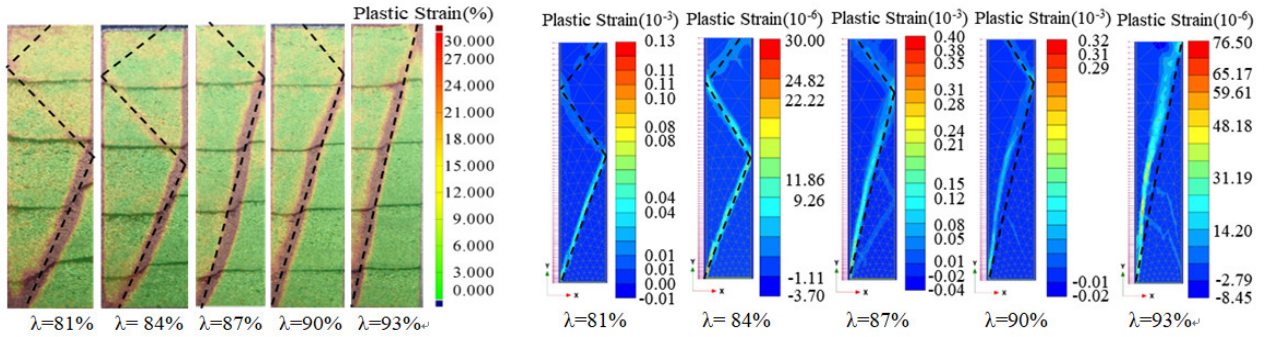

(a) Test results (b) Simulation result

Fig. 10 Influence of compaction degree on morphological characteristics of active fracture surface of finite soil(n=0.2)

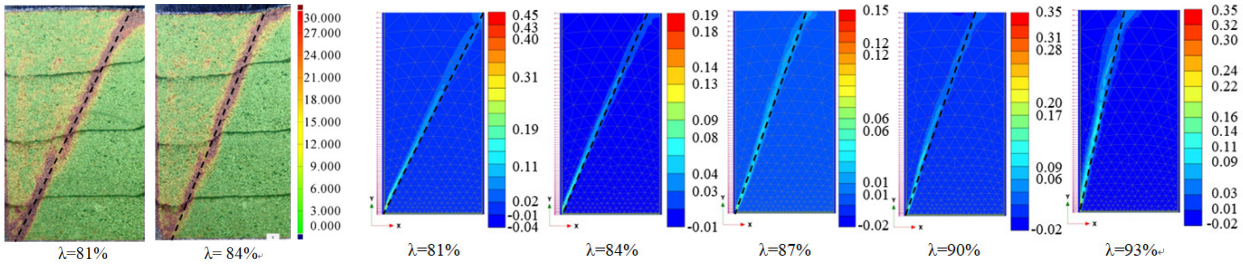

(a) Test results (b) Simulation result

Fig. 11. Influence of compaction degree on morphological characteristics of semi-infinite soil active fracture surface (n=0.5)

B. The Influence of Compaction Degree on the Morphological Characteristics of Active Fracture Surface

As shown in Fig. 10 and Fig. 11, taking the finite soil (n=0.2) and semi-infinite soil (n=0.5) with λ=81 % as examples, the influence of compaction degree on the morphological characteristics of the active fracture surface of TT mode is discussed.

It can be seen from Fig. 10 that the compaction degree has a significant effect on the morphological characteristics of the active fracture surface of finite soil under the TT mode; the test results are basically consistent with the simulation results. With the increase of compaction degree, the active fracture surface of finite soil with a certain width-height ratio under TT mode gradually changes from broken line to straight line, the number of broken line segments decreases from 3 to 1, and the finite soil gradually changes into semi-infinite soil.

It can be seen from Fig. 11 that the compaction degree has an effect on the morphological characteristics of the active fracture surface of semi-infinite soil under TT mode; the test results are basically consistent with the simulation results. With the increase of compaction degree, the active fracture surface of semi-infinite soil with a certain width-height ratio under TT mode becomes steeper and steeper, the active fracture surface dip angle increases gradually; the soil behind the wall is still semi-infinite.

C. The Influence of Compaction Degree on the Critical Width-Height Ratio of Finite soil

1) Morphological Characteristics of Active Fracture Surface of Fill with Different Compaction degree and Width-Height Ratio

Due to the limitation of test conditions, model tests under some working conditions are not carried out. The nine working conditions of the model test did not carry out are as follows: (1) λ=84%, n=0.6; (2) λ=87%, n=0.5, 0.6; (3) λ=90%, n=0.4, 0.5, 0.6; (4) λ=93%, n=0.4, 0.5, 0.6. The active fracture surfaces of the fill under the nine working conditions are obtained by numerical simulation. The results of the active fracture surface under the TT mode obtained by the test and numerical simulation are shown in Fig. 12.

It can be seen from Fig. 12 that: (1) The test results of the active fracture surface of different compaction degrees and different width-height ratios under the TT mode are basically consistent with the simulation results, the active fracture surface begins at the heel of the wall and ends at the surface of the fill. (2) When the degree of compaction is constant, with the increase of the width-height ratio of fill, the active fracture surface gradually changes from a broken line to a straight line, the dip angle of the fracture surface gradually decreases, the plane shape of the fracture body changes from 'trapezoid' to 'triangle'; the soil behind the wall gradually changes from a finite soil to a semi-infinite soil.

2) The Critical Width-Height Ratio of Fill with Different Compaction degree

Based on the morphological characteristics of the active fracture surface of fill under different working conditions shown in Fig. 12, the working conditions closest to the critical state in different width-height ratios under a certain degree of compaction are found. The determination method of critical width-height ratio is illustrated by taking the model test results of λ=81% as an example. As shown in Fig. 12(a), comparing the model test results with a compaction degree of 81% and a width-height ratio of 0.2, 0.3, 0.4, 0.5 and 0.6, it is found that when the n=0.5, the end point of the fracture surface moves to the vicinity of the intersection between the fixed retaining wall and the fill surface. At this time, the width-height ratio of the fill is about to reach the critical value, it can be speculated that the critical width-height ratio is slightly less than 0.5. As shown in Fig. 13, the width and height of the backfill are B and H respectively, and the horizontal projection of the backfill fracture surface is B', the critical width-height ratio can be calculated as n_{cr}=B'/H

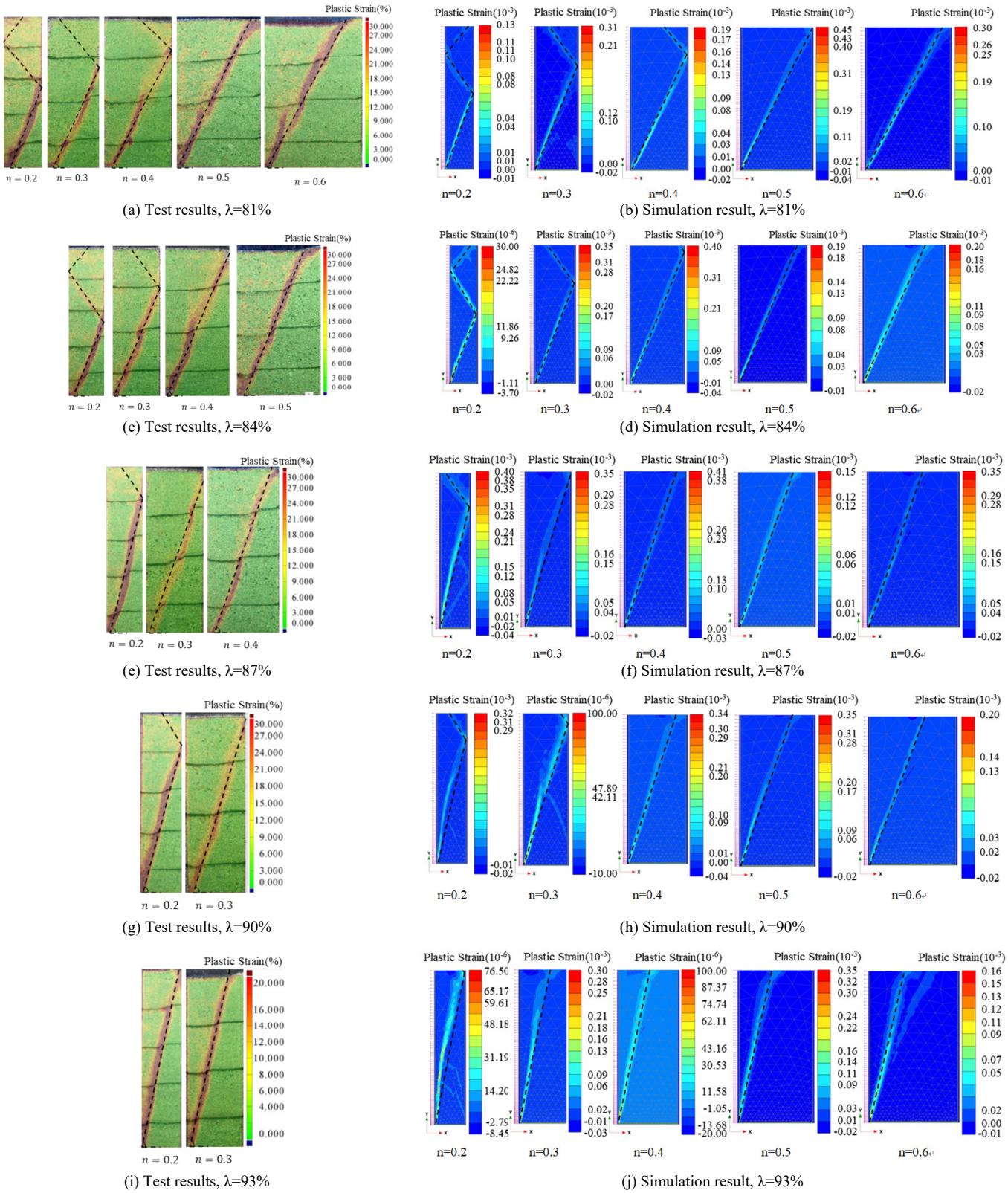

(a) Test results, λ=81%

(b) Simulation result, λ=81%

(c) Test results, λ=84%

(d) Simulation result, λ=84%

(e) Test results, λ=87%

(f) Simulation result, λ=87%

(g) Test results, λ=90%

(h) Simulation result, λ=90%

(i) Test results, λ=93%

(j) Simulation result, λ=93%

Fig. 12. Active rupture surface of fill with different compaction degree and different aspect ratio under TT mode

According to the above methods, the test and simulation values of the critical width-height ratio of fill with different compacts in TT mode are determined, as shown in TABLE VI.

It can be seen from TABLE VI that both the test and simulation values of the critical width-height ratio of the finite soil under TT mode decrease with the increase of the compaction degree of the fill. The difference between the test and simulation values of the critical width-height ratio under different compaction degrees is less than 15%. For the sand used in this paper, when the compaction degree increases from 81% to 93%, the test value of the critical width-height ratio decreases from 0.49 to 0.22, and the simulation value of critical width-height ratio decreases from 0.50 to 0.19. The fitting analysis of the test value and the simulation value is carried out respectively, and two relationship curves between critical width-height ratio and compaction degree under TT mode are obtained as shown in Fig. 14, the corresponding fitting equations of the test value and the simulation value is Eq. (3) and Eq. (4), respectively.

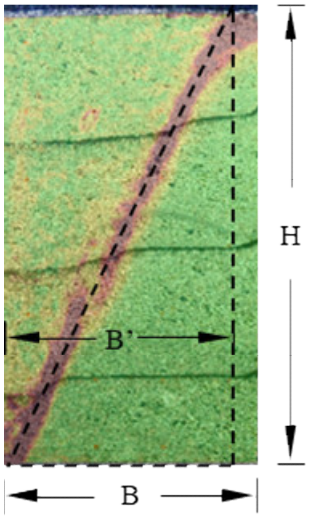

Fig. 13. Schematic diagram for determining the critical width-height ratio (λ=81%, n=0.5)

TABLE VI
CRITICAL WIDTH-HEIGHT RATIO TEST VALUE AND SIMULATION VALUE

Compaction degree λ(%)	Test value of critical width-height ratio n_{cr}^{T}	Simulation value of critical width-height ratio n_{cr}^{S}	Percentage difference between test value and model value (%)
81	0.49	0.50	1.09
84	0.45	0.42	7.25
87	0.37	0.34	8.93
90	0.30	0.33	7.94
93	0.22	0.19	14.61

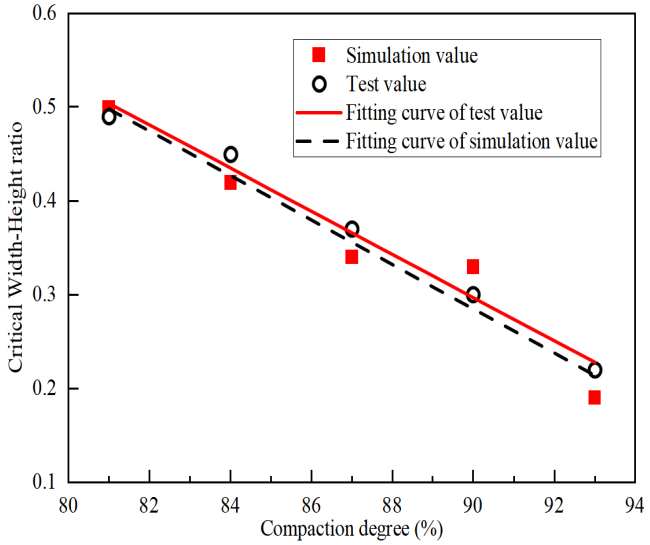

Fig. 14. Relationship curve between critical width-height ratio and compaction degree under TT mode

$$n_{cr}^{T} = -0.023\lambda + 2.367 \quad R^2 = 0.989 \tag{3}$$

$$n_{cr}^{S} = -0.024\lambda + 2.415 \quad R^2 = 0.945 \tag{4}$$

From the Eq. (3) and Eq. (4), it can be seen that the test value n_{cr}^{T} and the simulation value n_{cr}^{S} of the critical width-height ratio of the finite soil under TT mode decrease linearly with the increase of the compaction degree λ of the fill. The correlation degree R^2 is 0.989 and 0.945, respectively, which are highly linearly correlated.

VI. CONCLUSION

Through model tests and numerical simulations, the influence of compaction degree of fill behind the retaining wall on the active failure characteristics and the critical width-height ratio of finite soil under TT mode are studied. The experiment of the basic physical and mechanical index of fill material is carried out, the empirical relation between compaction degree and density, as well as the compaction degree and internal friction angle of fill materials is established. The dynamic development process and morphological characteristics of the active fracture surface of fill with different compaction degrees and width-to-height ratios are analyzed. A method to determine the critical width-to-height ratio of finite soil is proposed based on the fracture surface characteristics of the fill. Through comparative analysis, the experimental results are basically consistent with the simulation results, which indicate the reliability of the research results. The main conclusions are as follows:

(1) The dynamic development law of the active fracture surface of fill behind the wall under TT model is obtained. The active fracture surface of finite soil is a multi-section break line that starts at the heel of the wall and goes back and forth between the fixed retaining wall and the movable retaining wall, and ends at the fill surface. The active fracture surface of semi-infinite soil is approximately a straight line, starts from the heel of the wall, develops gradually along the diagonal line, and ends at the fill surface.

(2) The compaction degree of fill has a significant effect on the morphological characteristics of the active fracture surface under the TT mode. For the finite soil with a certain width-height ratio, with the increase of compaction degree, the active fracture surface gradually changes from broken line to straight line, the number of broken line segments gradually decreases, and the finite soil gradually changes into semi-infinite soil. For the semi-infinite soil with a certain width-height ratio, with the increase of compaction degree, the active failure surface becomes steeper and steeper and the volume of the fracture body decreases gradually, the soil behind the wall is still semi-infinite.

(3) The morphological characteristics of the active fracture surface under TT model vary with the change of the width-height ratio of the fill. When the compaction degree is constant, with the increase of the width-height ratio of fill, the active fracture surface of the fill gradually changes from a broken line to a straight line, the inclination angle of the fracture surface gradually decreases, the plane shape of the fracture body changes from 'trapezoid' to 'triangle', and the finite soil behind the wall gradually changes to semi-infinite soil.

(4) The compaction degree of fill has a significant impact on the critical width-height ratio of finite soil under active failure in TT mode. The critical width-height ratio of finite soil decreases linearly with the increase of compaction degree. For the sand used in this paper, when the compaction degree of the fill increases from 81% to 93%, the critical width-height ratio test value n_{cr}^{T} decreases from 0.49 to 0.22, and the critical width-height ratio simulated value n_{cr}^{S} decreases from 0.50 to 0.19. The empirical equation of critical width-height ratio test value n_{cr}^{T} and critical

width-height ratio simulated value n_{cr}^{S} considering the compaction degree λ are obtained as follows: $n_{cr}^{T} = -0.023\lambda + 2.367$ and $n_{cr}^{S} = -0.024\lambda + 2.415$, respectively. Both equations show a highly linear correlation.

This study explores for the first time the influence of compaction degree of backfill behind retaining walls on the morphological characteristics of fracture surfaces and the critical width-height ratio of finite soil, demonstrating that the compaction degree is an important factor affecting the critical width-height ratio of finite soil. This study contributes to understanding the deformation and failure mechanism of the finite soil behind the retaining wall, enriching the calculation theory of the finite soil pressure, and providing useful reference for designing and constructing the finite soil retaining structure, which has significant theoretical value and engineering practice significance.

REFERENCES

[1] W. S. Chen, Q. Y. Zhao, T. H. Ling, " Sliding surface mechanism of limit soil mass under classical Rankine earth pressure," Rock and Soil Mechanics, vol. 32, no. 12, pp 3571-3576, 2011.

[2] Y.Q. Zeng, J.W. Huang, Q.S. Hu, R.Y Zang, W.D. Hu, X.H. Liu, and H. Luo, " Sensitivity analysis of stability influencing factors for inverted t-type retaining wall in an active limit state based on strength reduction method and orthogonal experimental design," IAENG International Journal of Applied Mathematics, vol. 54, no. 11, pp 2253-2265, 2024.

[3] Y.Q. Zeng, W.D. Hu, M. X. Chen, Y. H. Zhang, X.H. Liu, X. N. Zhu, " Study on the failure characteristics of sliding surface and stability analysis of inverted t-type retaining wall in active limit state," Plos One, vol. 19, no. 2, pp 1-26, 2024.

[4] W. D. Hu, Y. Q. Zeng, X. N. Zhu, and T. Hu, "Determination of passive earth pressure on a cantilever retaining wall in a narrow foundation pit based on logarithmic spiral sliding surface," International Journal of Geomechanics, vol. 23, no. 8, pp 1-9, 2023.

[5] X. N. Zhu, Y. Q. Zeng, W. D. Hu, X. H. Liu, and X. Y. Zhou, "Experimental study on passive earth pressure against flexible retaining wall with drum deformation," Engineering Letters, vol. 29, no. 2, pp 339-350, 2021.

[6] X. N. Zhu, W. D. Hu, Y. Q. Zeng, T. Hu, S. Q. Jiang, and W. W. Wang. " Experimental study on deformation characteristics and active earth pressure against the flexible retaining wall with limited width soil in foundation pit," IAENG International Journal of Applied Mathematics, vol. 52, no. 4, pp 875-889, 2022.

[7] J. X. Hua, and J. G. Zheng, Geological engineering handbook, 5th edition. Beijing, China: China Building Industry Press, 2018.

[8] Y. Que, X. F. Gui, and F. Q. Chen, "Active earth pressure against cantilever retaining walls with a long relief shelf in rotation about the top," KSCE Journal of Civil Engineering, vol. 27, no. 6, pp 2463-2476, 2023.

[9] W. D. Hu, X. N. Zhu, Y.Q. Zeng, X. H. Liu, and C.C. Peng, " Active earth pressure against flexible retaining wall for finite soils under the drum deformation mode," Scientific Reports, vol. 12, no. 1, pp 1-25, 2022.

[10] Y. Wang, H. B. Chen, G. P. Jiang, and F. Q. Chen, "Slip-line solution for the active earth pressure of narrow and layered backfills against inverted t-type retaining walls rotating about the base," International Journal of Geomechanics, vol. 23, no. 5, pp 1-14, 2023.

[11] X.B. Dai, "Experimental study of active earth pressure of cohesionless soil with limited width behind the retaining wall and numerical simulation," M.S. thesis, Dept. Civil. Eng., Hunan Univ., Hunan, China, 2016.

[12] C. Y. Wang, X. P. Liu, Z. H. Cao, X. Jiang, and J. Q. Zhang, "Experimental study on characteristics of active slip surface of limited width soil behind rigid wall ," Rock and Soil Mechanics, vol. 42, no. 11, pp. 2943-2952, 2021.

[13] S. M. Yang, "Experimental research on active earth pressure of limited cohesionless soil under immersed," M.S. thesis, School of Civil Engineering and Architecture, East China Jiaotong University., Jiangxi, China, 2018.

[14] X. Jiang, "Experimental study of deformation and failure characteristics with limited width behind the retaining wall and numerical simulation," M.S. thesis, School of Hydraulic and Environmental Engineering, Changsha University of Science & Technology., Hunan, China, 2018.

[15] M. H. Yang, X. B. Dai, M. H. Zhao, and H. Luo, " Experimental study on active earth pressure of cohesionless soil with limited width behind retaining wall," Chinese Journal of Geotechnical Engineering, vol. 38, no. 1, pp 131-137, 2016.

[16] M. T. Xia, "Experimental analysis on mechanical characteristics of narrow backfill behind foundation pit diaphragm wall," Chinese Journal of Underground Space and Engineering, vol. 18, no. 2, pp 546–553, 2022.

[17] T. Fang, S. H. Sun, C. J. Xu, H. L. Wang, R. R. Yang, N. Wang, "Earth pressure experimental study of limited soil considering the mode of displacement of retaining wall," Journal of Railway Science and Engineering, vol. 16, no. 5, pp 1178–1185, 2019.

[18] M. H. Khosravi, T. Pipatpongsa, J. Takemura, "Experimental analysis of earth pressure against rigid retaining walls under translation mode," Géotechnique, vol. 63, no. 12, pp 1020-1028, 2013.

[19] Y.Y. Zhou, M.L. Ren, "An experimental study on active earth pressure behind rigid retaining wall," Chinese Journal of Geotechnical Engineering, vol. 12, no. 2, pp 19-26, 1990.

[20] W. Zhu, "Experimental and theoretical study on earth pressures considering finite soils and retaining wall deformation," M.S. thesis, Dept. Architectural. Eng., Zhejiang University., Zhejiang, China, 2014.

[21] D. Liu, "DEM analysis and simplified calculation of active earth pressure on retaining walls of narrow backfill width," M.S. thesis, Dept. Civil. Eng., Hunan Univ., Hunan, China, 2018.

[22] L. Wan, X.Z. Zhang, Y.F. Wang, L.M. Xu, C.J. Xu, "DEM study on active failure and earth pressure of cohesionless soil with limited width behind retaining wall," Journal of Civil and Environmental Engineering, vol. 41, no. 3, pp 19-26, 2019.

[23] H. Z. Zhang, C. J. Xu, L. J. Liang, S. L Hou, R. D. Fan, and G. H. Feng, "Discrete element simulation and theoretical study of active earth pressure against rigid retaining walls under RB mode for finite soils," Rock and Soil Mechanics, vol. 42, no. 10, pp. 2895-2907, 2021.

[24] H.Z. Zhang, C.J. Xu, Z.B. He, Z.J. Huang, X.H. He, "Study of active earth pressure of finite soils under different retaining wall movement modes based on discrete element method," Rock and Soil Mechanics, vol. 43, no. 1, pp. 257–267, 2022.

[25] H.Z. Zhang, "Study on Active Earth Pressure of Finite soils Under Different Retaining Wall Movement modes," M.S. thesis, Dept. Architectural. Eng., Zhejiang University., Zhejiang, China, 2022.

[26] D. Huang, "Study on Active Earth Pressure on Retaining Walls Adjacent to Existing Basement," M.S. thesis, Dept. Architectural. Eng., Zhejiang University., Zhejiang, China, 2010.

[27] F. Q. Chen, Y. J. Lin, D. Y. Li, "Solution to active earth pressure of narrow cohesionless backfill against rigid retaining walls under translation mode ," Soils and Foundations, vol. 59, no. 1, pp. 151-161, 2019.

[28] Y. H. Du, S. J. Pan, W. X. Fu, M. Jiang, Y. S. Li, M. Zhang, B. Huang, W.Z. Xu, "Effect of continuous heavy rainfall on the earth pressure of finite soil ," Science Technology and Engineering, vol. 22, no. 7, pp. 2806-2813, 2022.

[29] B. Jiang, H. W. Ying, K. H. Xie, "Study on earth pressure on silos based on soil arching ," Bulletin of Science and Technology, vol. 21, no. 5, pp. 624-627, 2005.

[30] P. Ma, S. Q. Qin, H. T. Qian, "Calculation of active earth pressure for finite soils," Chinese Journal of Rock Mechanics and Engineering, vol. 27, no. S1, pp. 3070-3074, 2008.

[31] X. X. Liu, B. Li, W. W. Wang, C. He, S. Li, "Calculation of active earth pressure of finite soil based on layered principal stress trajectory," Rock and Soil Mechanics, vol. 43, no. 5, pp. 1175-1186, 2022.

[32] F.W. Lai, S.Y. Liu, D .Y. Yang, Y. H. Cheng, Q. J. Fan, "Generalized solution to active earth pressure exerted onto retaining wall with narrow backfills," Chinese Journal of Geotechnical Engineering, vol. 44, no. 3, pp. 483-491, 2022.

[33] T .J. Shu, "Study on earth pressure of finite soil in foundation pit engineering," M.S. thesis, Dept. Architecture. Eng., Nanchang University., Jiangxi, China, 2020.

[34] Y. Wei, "Calculation and application of active earth pressure on finite soil behind wall," M.S. thesis, College of Architecture and Civil Engineering, Xi`an University of Science and Technology., Xi`an, China, 2020.

Dr. Xiaohong Liu received the Ph.D. degree from Central South Univesrtiy, Changsha, China, in 2011. She is the professor of College of Civil Engineering and Architecture, Hunan Institute of Science and Technology, Yueyang, China. Her research interests cover excavation engineering and earth pressure and non-contact testing of foundation deformation. She has published more than 30 technical papers.

Yuchen Liu received his B.E. degree from Southwest Jiaotong University, Chengdu, China, in 2020. In 2022, he entered Hunan Institute of Science and Technology for a master's degree. He is mainly engaged in geotechnical engineering research.

Dr. Zhengfu Liu was born in May 1990 and received his M.S.Degree from Central South University, Changsha, China, in 2015, and received the Ph.D. degree from Changsha University of Science & Technology, Changsha, China, in 2023. His research interests are mainly on geotechnical engineering. He is a lecturer in College of Management, Hunan City University, Yiyang, China. He authored or co-authored 12 journal papers.

Dr. Yongqing Zeng was born in February 1991 and received his M.S.Degree from Anhui University of Science and Technology, Huainan, China, in 2016, and received the Ph.D. degree from Institute of Rock and Soil Mechanics, Chinese Academy of Sciences, Wuhan, China, in 2019. His research interests are mainly on geotechnical engineering. He is an associate professor in College of Civil Engineering and Architecture, Hunan Institute of Science and Technology, Yueyang, China. He authored or co-authored 25 journal papers and 5 international conference papers.

Yuxin Wang was born in September 1999 and received his B.E.degree from Shanxi University, Taiyuan, China, in 2022. In the same year, he entered Hunan Institute of Science and Technology for a master's degree. He is mainly engaged in geotechnical engineering research.

Sanxian Liu was born in February 1987 and received his B.E.degree from Guizhou University, Guizhou, China, in 2010. After graduating from college, he has been engaged in geotechnical engineering investigation and design work in Yueyang Baili Survey Technology Co., Ltd. of Hunan Province.